\$ SUPER

Contents lists available at ScienceDirect

# Journal of Biomechanics

journal homepage: www.elsevier.com/locate/jbiomech





# Impact of model geometry and joint center locations on inverse kinematic/dynamic predictions: A comparative study of sexually dimorphic models

Joseph Dranetz<sup>1</sup>, Shuo Chen<sup>1</sup>, Hwan Choi \*

Department of Mechanical and Aerospace Engineering, Biionix Cluster, University of Central Florida, 6900 Lake Nona Blvd, Orlando, FL, United States

#### ARTICLE INFO

# Keywords: Computational musculoskeletal modeling Sexually dimorphism Functional joint center testing Gait analysis Body segment inertial properties

#### ABSTRACT

This work illustrates the sensitivity of demographically characteristic body segment inertial properties and subject-specific customization on model performance. One characteristic demographic, gender, and one subjectspecific characteristic, hip joint center location, were represented with musculoskeletal modeling to evaluate how design decisions may alter model outputs. Generic sexually dimorphic musculoskeletal models were developed from the commonly used Rajagopal model using male and female data adapted by Dumas et al. Hip joint centers of these models were adjusted based on functional joint center testing. The kinematics and dynamics of 40 gait cycles from four subjects are predicted using these models. Two-way analysis of variance (ANOVA) was performed on the continuous time series data using statistical parametric mapping (SPM) to assess changes in kinematics/dynamics due to either choice in model (Rajagopal vs Dumas) or whether joint center adjustment was performed. The SPM based two-way ANOVA of the inverse dynamics found that differences in the Rajagopal and Dumas models resulted in significant differences in sagittal plane moments during swing (0.115  $\pm$  0.032 Nm/kg difference in mean hip flexion moment during initial swing and a 0.077  $\pm$  0.041 Nm/kg difference in mean hip extension moment during terminal swing), and differences between the models with and without hip joint center adjustment resulted in significant differences in hip flexion and abduction moments during stance (0.217  $\pm$ 0.055 Nm/kg increased mean hip abductive moment). By comparing the outputs of these differently constructed models with each other, the study finds that dynamic predictions of stance are sensitive to positioning of joint centers, and dynamic predictions of swing are more sensitive to segment mass/inertial properties.

#### 1. Introduction

Quantitative analysis of human movement is desirable as it precisely describes human motion, but invasively obtaining the requisite data is often impractical in studies involving unimpaired or pathologic populations (Holder et al., 2020; Seth et al., 2011). Musculoskeletal modeling offers a non-invasive method for quantifying various biomechanical data. These subject-specific musculoskeletal models (MSM's) rely on linear scaling methods. However, modifications to joint parameters and body segment inertial parameters (BSIP's), masses, mass centers, and moments of inertia, made with linear scaling may distort some parameters unless the subject's anthropometrics align closely with those of the generic model (Koller et al., 2021; Lund et al., 2015). Due to differences in bone and muscle morphology, linear scaling may not accurately represent internal properties such as joint center locations or BSIP's. The reliability of using musculoskeletal modeling for movement

analysis significantly decreases when there is a mismatch between the anatomical characteristics of the linearly scaled generic model and those of the target participant (Correa et al., 2011; Kainz et al., 2021; Blemker et al., 2007; Miehling, 2019; Chambers et al., 2010).

Previous studies have developed generic multi-body MSM's, which have been widely used in biomechanical research (Seth et al., 2011; Delp, et al., 2007). Rajagopal et al. developed a full-body MSM representing a 75 kg, 170 cm tall male (Rajagopal, et al., 2016). This model integrates the Hamner full-body model, Arnold lower limb model and the Delp Gait2392 model (Hamner et al., 2010; Delp, et al., 1990; Arnold et al., 2010). The upper limb mass properties of this model are based on scans conducted by de Leva et al. on 100 male and 15 female Caucasian young adults (De Leva, 1996; Zatsiorski et al., 1990). Dissimilarly, the lower limb mass properties are derived from average anthropometric data measured by Anderson on five male subjects (Anderson & Pandy, 1999). Although previous research suggests that BSIP's have only a

E-mail addresses: joseph.dranetz@ucf.edu (J. Dranetz), shuo.chen@ucf.edu (S. Chen), hwan.choi@ucf.edu (H. Choi).

<sup>\*</sup> Corresponding author.

 $<sup>^{1}</sup>$  Co-first author.

Table 1
Subject Demographics and Lateral/Anterior Hip Joint Center Adjustments.

	Demographic Information				Lateral Hip Adjustment		Anterior Hip Adjustment	Anterior Hip Adjustment		
ID	Sex	Age Height (cm) Weight (kg)		Rajagopal model (cm)	Dumas model (cm)	Rajagopal model (cm)	Dumas model (cm)			
1	F	20	161	47.46	2.93	1.65	0.93	2.29		
2	F	24	157	55.74	4.09	2.81	2.4	4.15		
3	M	29	162	54.6	3.24	2.36	1.62	2.94		
4	M	21	190	94.78	3.25	2.08	0.84	3.41		

minor effect on kinetic analysis outcomes (Wesseling et al., 2014), the International Society of Biomechanics (ISB) has emphasized that incorrectly applying BSIP's from different sources can introduce errors in inverse dynamics analysis (Derrick et al., 2020). This highlights the importance of using female BSIP's when modeling female subjects.

Clinical imaging techniques can accurately estimate subject-specific BSIP's (Kudzia et al., 2022; Cizgin et al., 2017; Peyer et al., 2015). However, aggregating these measurements to create demographicspecific models is limited by insufficient sampling of diverse populations. Several studies have characterized populational differences by constructing an anatomical atlas, which amasses and categorizes the data of a diverse set of individuals from which one can be selected in the development of a demographic-specific model (Zhang et al., 2016; Ding et al., 2019; Fernandez et al., 2023; Toderita et al., 2021). However, the extent to which implementation of demographic-specific models might improve model accuracy is not well understood. Another conventional method for determining BSIP's are regression equations based on average data obtained from larger sample studies (De Leva, 1996; Clauser et al., 1969; McConville et al., 1980). In this approach, BSIP's are estimated based on segment length, which is determined through anthropometric measurements. Acknowledging the problem of inconsistent segment definitions for gendered BSIP's, Dumas et al. (Dumas et al., 2006) adjusted the BSIP regression equations from male (McConville et al., 1980) and female (Young et al., 1983) data to be expressed directly in conventional ISB recommended segment coordinate systems (Wu et al., 2005), as well as redefined the segment lengths based on joint centers. This adjustment makes it a valuable resource for creating generic gendered MSM's with appropriately defined segment frames and joint coordinates.

While BSIP's from Dumas et al. look to be suitable for MSM development, a potential improvement to the BSIP data is recognized: hip joint center (HJC) location. Determining the HJC location is crucial for various purposes such as creating segment frames, scaling BSIP's, and calculating kinematics. Dumas et al. used a regression equation method developed by Reed et al. for determining the HJC location based on models of automobile occupant posture (Reed et al., 1999). Previous studies have found that regression equations for determining HJC location have low reliability compared to functional or imaging methods, resulting in deviations of up to 3 cm (Kainz et al., 2015; Kainz, et al., 2017; Ehrig et al., 2006; Sangeux et al., 2014; Fiorentino, et al., 2016; Puchaud, et al., 2020). To overcome this limitation, a functional joint center localization approach like Symmetrical Center of Rotation

**Table 2**Inverse Kinematics Root Mean Square Error (RMSE).

Model Type	Subject 1	Subject 2	Subject 3	Subject 4	Model Average
Unadjusted Rajagopal (RU)	1.62 cm	1.62 cm	1.46 cm	1.45 cm	1.53 cm
Adjusted Rajagopal (RA)	1.72 cm	1.70 cm	1.71 cm	1.71 cm	1.71 cm
Unadjusted Dumas (DU)	1.91 cm	1.94 cm	1.45 cm	1.48 cm	1.69 cm
Adjusted Dumas (DA)	2.28 cm	2.39 cm	1.88 cm	1.71 cm	2.07 cm
Subject Average	1.88 cm	1.91 cm	1.62 cm	1.59 cm	1.75 cm

Estimation (SCoRE) can be adopted to locate the HJC. While SCoRE has shown effectiveness in in vivo applications (Ehrig et al., 2006), many other functional methods have been developed, some of which may produce more accurate results (Kainz et al., 2015). Recent studies have highlighted the importance of joint centers as virtual markers for accurate linear scaling of the femur and pelvis (Kainz, et al., 2017; Puchaud, et al., 2020; Koller et al., 2021; Lund et al., 2015). Determining the precise HJC location is crucial for establishing the local coordinate system of the hip joint, which directly influences the accuracy of modeled kinetics. Therefore, it is important to investigate the relationship between HJC adjustments based on functional joint center localization and their impact on modeling, particularly in conjunction with the implementation of gender-specific BSIP's.

Presently there is a need for MSM's that more accurately represent the bodies of individuals of varying morphology, age, gender, and race. Current models based primarily on small samples of healthy adult male data are not suitable for representing individuals outside these specific demographics (Correa et al., 2011; Kainz et al., 2021; Blemker et al., 2007; Miehling, 2019; Chambers et al., 2010). The purpose of this work was to generate gendered generic MSM's using demographic data and implement a subject specific customization onto them in the form of HJC adjustment to illustrate the sensitivity of demographically characteristic BSIP's and HJC location on model performance. By selecting one characteristic demographic to alter full model BSIP's from, gender, and one specific characteristic to adjust based on subject specific data, HJC location, we have introduced an avenue for exploring the nature of MSM's and how design decisions may alter model outputs. We anticipate the gendered BSIP's will cause general changes throughout the kinematic and dynamic results with stronger effects found with the female subjects as the original model used was based on primarily male data. Conversely, we anticipated that HJC adjustment would primarily affect hip kinematics and dynamics.

## 2. Methods

In following ethical practices for research involving human subjects, all procedures, including the process for obtaining informed written consent, were approved by the University of Central Florida's Institutional Review Board. Segment BSIP data and anatomical landmark/joint center location data from the Dumas study were combined to generate sexually dimorphic generic MSM's: the Dumas models. The models were adapted from a generic Rajagopal model, altering the segment masses, center of mass locations, and moment of inertias to match the Dumas data. The joint definitions were moved to match the Dumas joint center locations, and the Dumas anatomical landmarks were used to define new marker positions. Tables comparing the segment BSIP's, joint center locations, and anatomical landmark locations of the Rajagopal model and the two gendered Dumas models can be found in the appendix (Tables 4–8).

Data from 4 adults (2 male and 2 female) were used to develop models and evaluate their ability to represent subject specific gait kinematics and dynamics (Table 1). Subjects wore a set of 46 reflective markers following a modified Helen-Hayes set (Kadaba et al., 1990), tracked at 100 Hz by a 12 infrared camera motion capture system (Vero, Vicon, Yarnton, UK). Force plates (Optima, AMTI, Watertown, MA) were used to measure the ground reaction forces at 2000 Hz. First, subjects

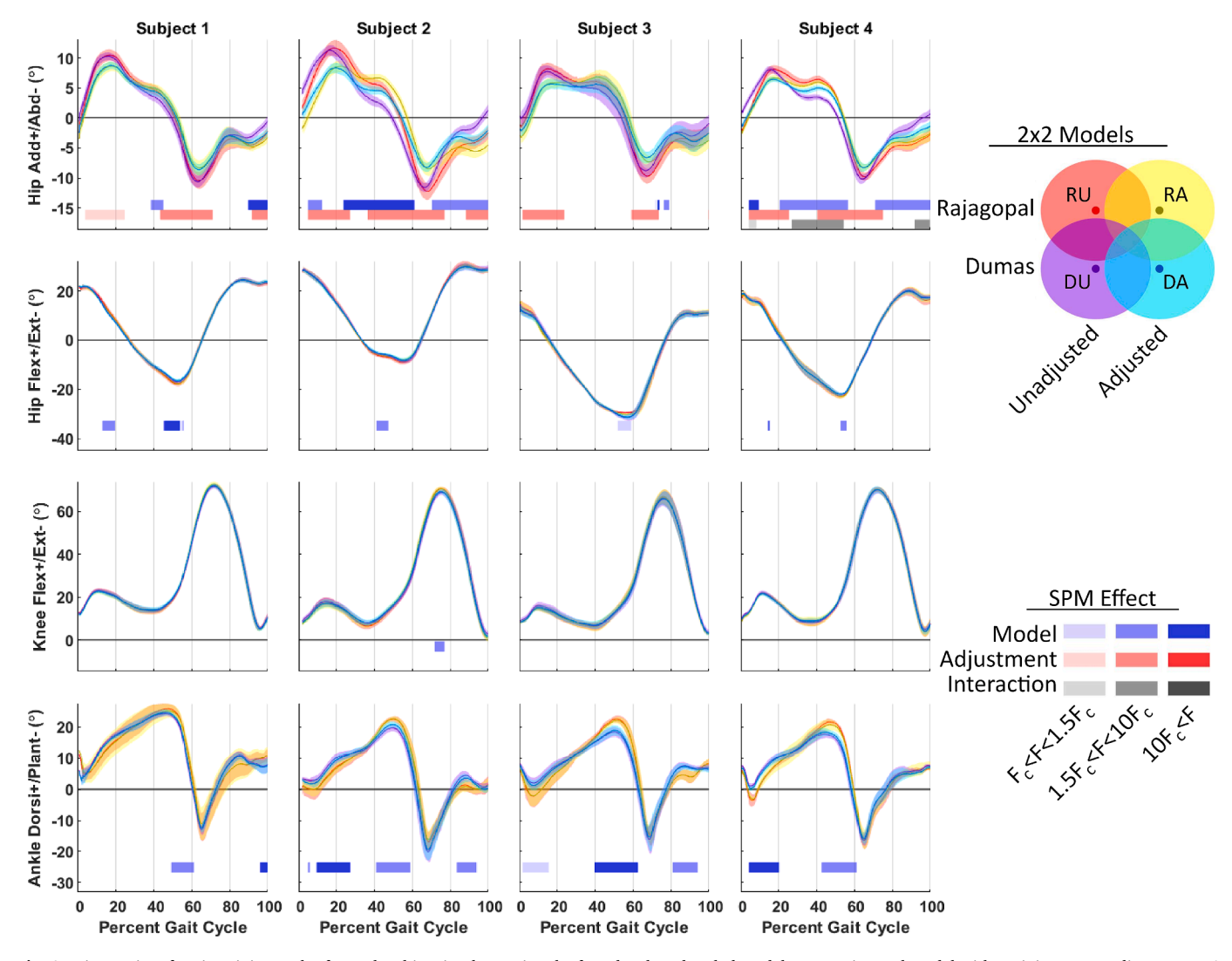


Fig. 1. Kinematics of various joint angles for each subject implementing the four developed scaled models. RU: Rajagopal model without joint center adjustment, RA: Rajagopal model with joint center adjustment, DU: Dumas model without joint center adjustment, and DA: Dumas model with joint center adjustment. Shaded regions represent the area of  $\pm 1$  standard deviation. The colored boxes below each plot represent regions in the gait cycle identified as having significant differences due to model effects (blue), joint center adjustment effects (red), or interaction effects of the two (grey).

executed a 'StarArc' movement pattern, conducive for functional joint center testing (Camomilla et al., 2006; Ehrig et al., 2006). Next, subjects performed walking trials across two force plates in the center of a 14 m walkway. Only passes with complete and isolated foot contact onto each force plate were accepted into the study data set. Data from the first 10 valid passes (5 led with each foot) of each subject were implemented in the MSM's. A consequence of the experimental setup only including two consecutive force plates in the walkway was that ground reaction forces of complete gait cycles were not collected (only  $\sim$  90 % of the gait cycle from toe off to ipsilateral heel strike).

For each subject, both a generic Rajagopal model and the corresponding generic Dumas model were scaled in OpenSim using scale factors similarly defined with marker trajectory data from a static portion of the functional joint center testing trial. For scaled Rajagopal and Dumas models of each subject, the difference between the models' original HJC and those predicted by functional joint center estimation (SCoRE) were measured. To perform the joint center adjustment without disrupting model scaling, the joint centers were proportionately adjusted in the generic model and the models were scaled again with the same scaling settings. The adjustments made to the HJC's of each model are documented in Table 1.

Inverse kinematics and inverse dynamics were performed on the 16

models (4 subjects x 2 generic models x 2 with/without HJC adjustment) with the walking trial data. All data was temporally normalized by gait cycle. Kinematic data was de-meaned to account for differences in model coordinate definitions, and dynamic data was normalized by subject mass. Two-way analysis of variance (ANOVA) was performed using statistical parametric mapping (SPM) (Pataky et al., 2016) to assess changes in kinematics/dynamics due to either model choice (Rajagopal vs Dumas) or whether HJC adjustment was performed. The SPM two-way ANOVA was performed for each subject individually, for groups separated by gender, and for the whole dataset to assess inter-subject variance as well as highlight any gender effects. Fig. 4 found in the Appendix summarizes the methods for model generation, data processing, and data analysis.

SPM based tests for equal variance (Kowalski et al., 2021) and normality (D'Agostino-Pearson K-squared) (D'Agostino et al., 1990) were performed to test ANOVA assumptions. Finally, post hoc pairwise t tests were performed with a Bonferroni correction factor to validate results from the two-way ANOVA. In order to evaluate the gendered effects of the Dumas models independent of the differing coordinate system definitions of the Rajagopal and Dumas models, Dumas models representing the opposite sex of each subject were scaled, inverse kinematics and inverse dynamics was performed using the same marker

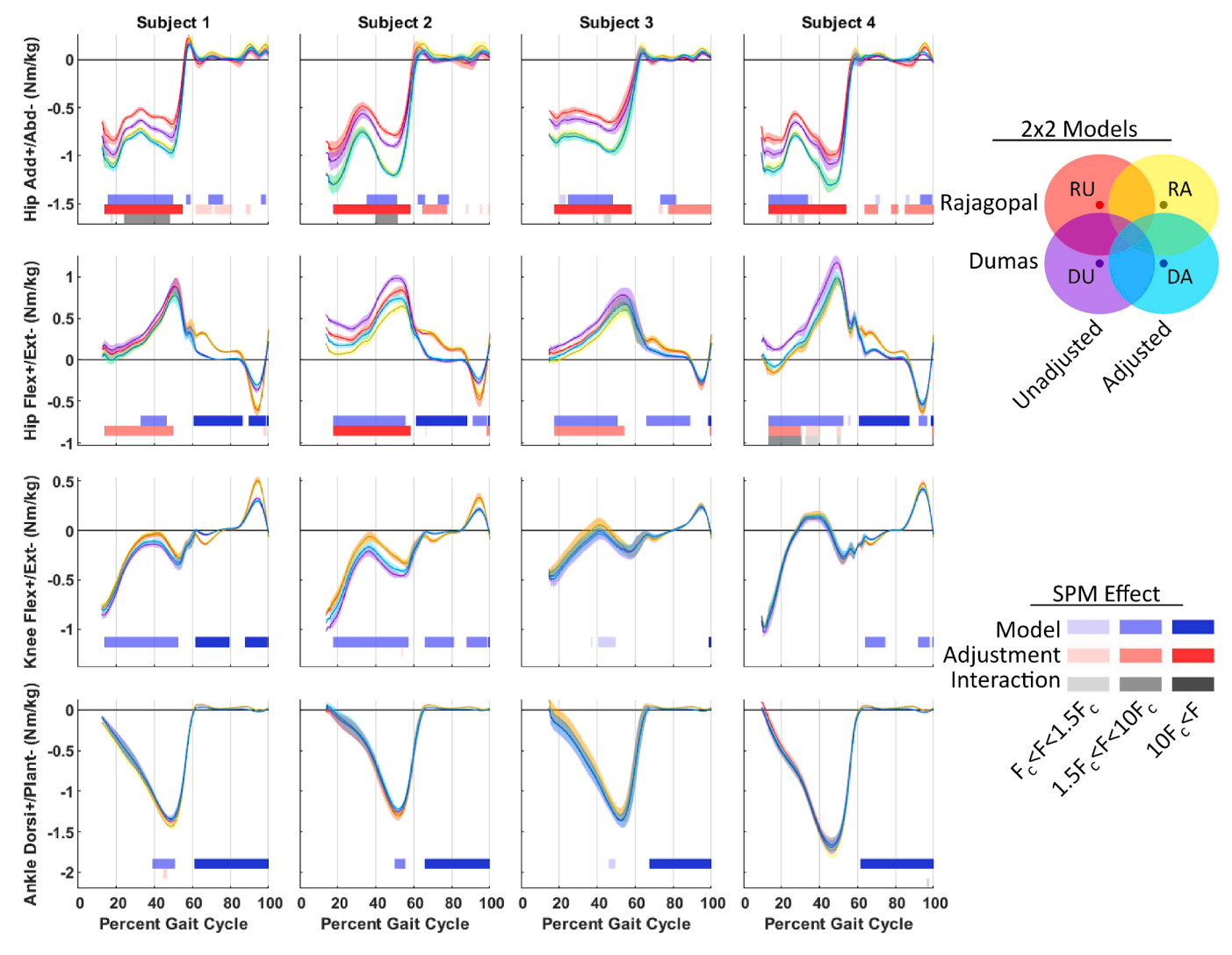


Fig. 2. Dynamics of various joint moments for each subject implementing the four developed scaled models. RU: Rajagopal model without joint center adjustment, RA: Rajagopal model with joint center adjustment, DU: Dumas model without joint center adjustment, and DA: Dumas model with joint center adjustment. Shaded regions represent the area of  $\pm 1$  standard deviation. The colored boxes below each plot represent regions in the gait cycle identified as having significant differences due to model effects (blue), joint center adjustment effects (red), or interaction effects of the two (grey).

trajectory and ground reaction force data, and an SPM based one-way ANOVA was performed.

#### 3. Results

Marker root mean square error (RMSE) ranged between 1.45 cm and 2.39 cm for the inverse kinematic operations (Table 2) with the Rajagopal models having lower marker RMSE's and models with HJC adjustment having higher marker RMSE's for the inverse kinematic operations.

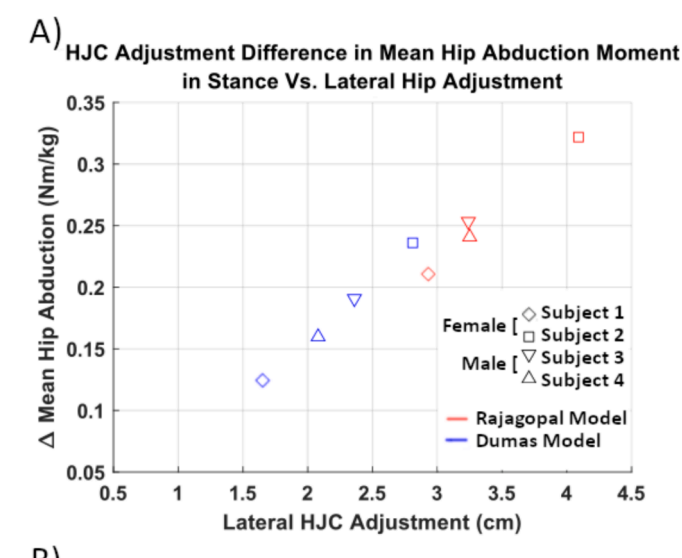
Statistically meaningful differences in sagittal plane kinematics were found between the Rajagopal and Dumas models occurring primarily at the ankle, with a  $2.27\pm1.61^\circ$  higher peak dorsiflexion in late stance for the Rajagopal models (Fig. 1). Statistically significant differences in hip adduction/abduction were found to be due to both model effects and joint center adjustment effects. The joint center adjustments led to smaller magnitude adductive and abductive excursions: smaller maximum adductions in early stance and smaller maximum abductions in early swing. Combined, the joint adjusted models predicted a  $4.42\pm1.91^\circ$  smaller span across the motion.

The SPM based two-way ANOVA identified two modelling effects on inverse dynamics: Use of either the Rajagopal or Dumas model resulted

in differences in sagittal plane moments during swing, and the addition of HJC adjustment to the models resulted in differences in hip flexion and abduction moments during stance (Fig. 2). The Rajagopal models showed a  $0.115\pm0.032$  Nm/kg larger mean hip flexion moment during initial swing and a  $0.077\pm0.041$  Nm/kg larger mean hip extension moment during terminal swing. Additionally, the Rajagopal models showed a  $0.059\pm0.024$  Nm/kg larger mean knee flexion moment in terminal swing and a  $0.019\pm0.004$  Nm/kg larger mean ankle dorsiflexion moment throughout swing.

While the unadjusted Dumas models showed a 0.101  $\pm$  0.052 Nm/kg larger mean hip abductive moment compared to the unadjusted Rajagopal models during stance, adjusting both models' HJC locations increased the mean hip abductive moment in stance by 0.217  $\pm$  0.055 Nm/kg. In contrast, while the unadjusted Dumas models showed a 0.115  $\pm$  0.053 Nm/kg larger mean hip flexion moment compared to the unadjusted Rajagopal models during stance, adjusting both models' HJC locations decreased the mean hip flexion moment in stance by 0.113  $\pm$  0.052 Nm/kg. Despite initially predicting different hip abductive and flexion moments in stance, after HJC adjustment, the Rajagopal and Dumas models predicted similar moment trajectories.

Despite high intersubject variability relative to intrasubject variability, each individual subject SPM analysis reproduced similar effects



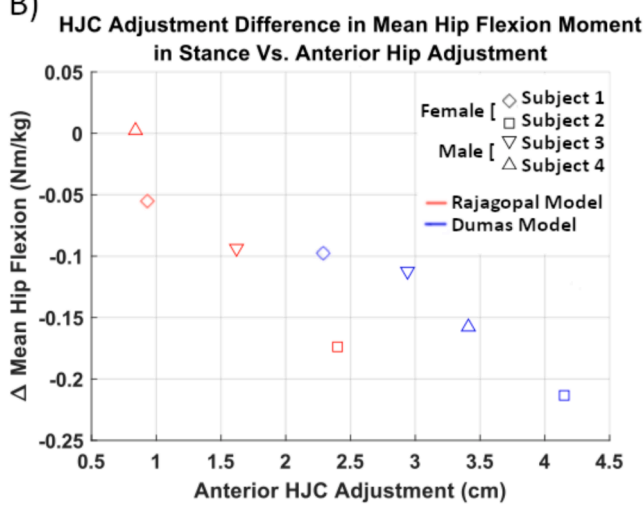


**Fig. 3.** The difference in mean hip abduction in stance is defined as the difference in average hip abduction moment (scaled by subject mass) from 0% to 60% gait cycle between a model before and after HJC adjustment. This difference is plotted against the lateral HJC adjustment of each model of each subject (A). The difference in mean hip flexion in stance is defined as the difference in average hip flexion moment (scaled by subject mass) from 0% to 60% gait cycle between a model before and after HJC adjustment. This difference is plotted against the anterior HJC adjustment of each model of each subject (B).

observed in the whole dataset analysis. SPM two-way ANOVA was repeated on each gender group (female: subjects 1 and 2, male: subjects 3 and 4). Several differences were identified with this analysis, the results of which are summarized in Table 3.

The SPM test for equal variance held in all regions where statistically significant differences in any group were identified. While the D'Agostino-Pearson K-squared test for normality rejected the null hypothesis for hip flexion/extension moment data throughout swing and hip adduction/abduction moment data throughout stance, performing the tests with each subject's data individually greatly reduced the regions of statistical significance. The largest remaining region of test failure occurred around 60 % of the gait cycle for each subject for both hip flexion/extension moment and hip adduction/abduction moment. The pairwise post hoc *t* test results largely corroborated the results from the SPM two-way ANOVA.

The one-way ANOVA comparing the application of each gendered Dumas model found that the predicted joint kinematics were very similar (Fig. 5 in Appendix), but the sagittal plane moments during swing differed (Fig. 6 in Appendix).

Table 3

Select differences between models for separate female and male data. Differences are described as either due to the HJC adjustment or due to use of the gendered generic model (based on the data reported by Dumas et al.  $\dagger$  indicates a non-significant effect where the mean effect was not more than one standard deviation away from zero.

	Female Models (Subjects 1, 2)	Male Models (Subjects 3, 4)
Reduction in hip adduction/abduction excursion due to HJC adjustment	$5.14\pm2.03^{\circ}$	$3.70\pm1.79^{\circ}$
Increase in hip abductive moment in	$0.223\pm0.056$	$0.211 \pm 0.054$
stance due to HJC adjustment	Nm/kg	Nm/kg
Reduction in hip flexion moment in	$0.135\pm0.048$	$0.090 \pm 0.055$
stance due to HJC adjustment	Nm/kg	Nm/kg
Reduction in hip flexion moment in	$0.144\pm0.027$	$0.086\pm0.038$
initial swing with Dumas model	Nm/kg	Nm/kg
Reduction in hip extension moment in	$0.137\pm0.041$	$0.016\pm0.041$
late swing with Dumas model	Nm/kg	Nm/kg †
Increase in knee extension moment in	$0.099 \pm 0.040$	$0.040 \pm 0.060$
stance with Dumas model	Nm/kg	Nm/kg †
Decrease in knee extension moment in	$0.40\pm0.018~\text{Nm}/$	$0.017 \pm 0.026$
initial swing with Dumas model	kg	Nm/kg †
Decrease in knee flexion moment in late	$0.102\pm0.025$	$0.016\pm0.024$
swing with Dumas model	Nm/kg	Nm/kg †
Difference in ankle moment in swing	$0.019\pm0.003$	$0.019\pm0.005$
due to model choice	Nm/kg	Nm/kg

#### 4. Discussion

This study's analyses indicated that the implementation of MSM's with gendered BSIP and joint definitions affected kinematic predictions of peak ankle dorsiflexion preceding push off and sagittal plane dynamics during swing, while HJC adjustment based on functional joint testing affected hip adduction/abduction kinematics and dynamics as well as hip flexion/extension dynamics during stance. The study found larger kinematic/dynamic changes with the female subject's, of which, the sagittal plane dynamics in swing can be attributed to use of the gendered Dumas model specifically. Although model predictions were not directly compared to measured kinematics/dynamics and the sample size was too small to make population-wide generalizations, this study demonstrated the sensitivity of MSM BSIP's and HJC location on predicted kinematics and dynamics of gait as well as highlighted the need for musculoskeletal modeling that accounts for the characteristic sexual dimorphisms of males and females.

The effects of the altered BSIP's observed in this study generally agreed with previous analyses assessing parameter sensitivity. Nguyen et al. varied BSIP's with Monte Carlo simulations demonstrating they had little effect on joint moments in gait with exception found during the swing phase. Additionally, they identified the effects of distal body BSIP's on proximal joint moments to be particularly small (Nguyen and Reynolds, 2014). Myers et al. expanded these Monte Carlo simulations, investigating both kinematics and dynamics. They similarly found the effect of modulating BSIP's more pronounced during swing, but contrarily identified foot mass as a dominant contributor to changes in hip flexion moment (Myers et al., 2015). While our study did not assess the effects of individual segment mass/inertial properties in isolation, rather whole body BSIP changes representing sexual dimorphism, the effects of altered BSIP's fit expectation with the more proximally distributed masses of the Dumas models predicting smaller peak joint moments during swing.

The comparison of the Rajagopal to Dumas models may conflate effects of altered BSIP's with the effects of the alternative coordinate definitions/joint center locations that the different models implement. The predicted kinematics and dynamics using both the male and female Dumas models with the same experimental data were compared to better isolate the effects of the sex-specific model properties. The oneway ANOVA from this analysis showed minimal effects on kinematics, likely due to the gendered Dumas models having similar joint/

coordinate definitions compared to the Rajagopal model, but pronounced dynamic effects during swing, indicating an effect of differing BSIP's. Congruent with previous work (Myers et al., 2015), Dumas models were found to be foot mass dominated: the smaller foot and shank percent segment masses but higher thigh percent segment mass of the female model resulted in overall smaller sagittal joint moments during swing compared to the male model.

HJC adjustment affected hip kinematics most dramatically while the use of the Dumas model's alternative joint definitions altered kinematics more generally. The HJC adjustment had a larger effect on hip abduction/adduction kinematics than on flexion/extension kinematics, a result in conflict with the previous work of Stagni et al. which identified more hip flexion/extension sensitivity with iterative inverse kinematics and dynamics on models with  $\pm$  30 mm HJC adjustments. This may have been due to SCoRE predicting lateral and anterior HJC adjustments, while Stagni et al. found superior/inferior HJC adjustments led to the largest changes in hip flexion/extension (Stagni et al., 2000). The largest differences in kinematics due to use of the gendered Dumas model compared to the Rajagopal model were found in hip abduction/adduction and ankle plantarflexion/dorsiflexion. These kinematic differences were likely due to differences in joint definitions between the models. For example, the Dumas model defined the ankle joint center as the midpoint of the malleoli found with a stereo-photogrammetric technique (Dumas et al., 2006), whereas the Rajagopal model defined the ankle based on the work of Inman et al. (Rajagopal, et al., 2016; Inman, 1976).

The effects of the HJC adjustment on dynamics fit expectations from previous work. Langenderfer et al. found that uncertainties in joint definitions had a larger impact on inverse dynamic predictions of stance compared to uncertainties in BSIP's (Langenderfer et al., 2008). Our study found larger lateral HJC adjustment (based on SCoRE prediction) led to increases in hip abductive moment in stance, while more anteriorly placed HJC's led to decreases in hip flexion moment in stance (Fig. 3), in agreement with the previous work of Stagni et al. (Stagni et al., 2000.

This investigation of model construction was successful at demonstrating the potential consequences of model design decisions on estimated kinematics and dynamics. Data was consistent with the assessment that choice in joint center location affected lower limb kinematics as well as the dynamics of stance while choice in mass/inertial segment properties influenced the dynamics of swing (Camomilla et al., 2017; Krabbe et al., 1997; Rao et al., 2006; Ganley & Powers, 2004). Quantifying the effect these sorts of alterations have on estimations of lower limb dynamics is an important target for computational biomechanists as it is currently unclear which alterations should be considered in model design (Moissenet et al., 2017).

The general efficacy of the two distinctly gendered models using the gendered data collected by Dumas et al. was more difficult to substantiate. While some of the characteristic effects of Dumas models on dynamics in swing were more pronounced for the models of the female subjects, e.g. hip and knee flexion/extension moments, other model outputs showed no gendered effect. While the true mass/inertial properties of the female segments should theoretically be closer to those

predicted by the Dumas model because of their use of female data, with a sample size of 4, the study at present cannot show the observed trends extend to humans generally.

As the accuracy of musculoskeletal modeling improves, the task of the computational biomechanists shifts from generating the most accurate model possible to generating one that is sufficiently accurate while minimizing resources used. While methods for generating highly accurate subject specific MSM's using magnetic resonance imaging data from the subject have been developed (Zhang, et al., 2014; Valente et al., 2017; Modenese & Renault, 2021), the acquisition and processing of these data is not always practical. For this reason, the development of demographically specific generic MSM's may provide a useful compromise between subject specific models and current generic models.

This study demonstrates the effects of model design choices on model performance as well as identifies a potential weakness in the use of models that do not account for sexually dimorphic characteristics of its subject data. Specifically, the study finds that the mischaracterization of joint center locations may alter the dynamics of stance, while the mischaracterization of segment mass/inertial properties is more likely to alter dynamic predictions of swing. Given that women tend to have more laterally placed hip joint centers (Dumas et al., 2006; Abd-Eltawab, et al., 2022), they would have larger hip abductive moments in stance which may be overlooked with current standard modeling techniques. These larger abductive moments may be part of the mechanistic explanation for the development of greater trochanteric pain syndrome, a condition with a prevalence 4 times greater in women (Sunil Kumar et al., 2021). Examples like this highlight the need for appropriate consideration of the anthropometric data sources that musculoskeletal models rely on. Representing characteristic differences between population groups is necessary in the future development of these models in order to represent individual subjects more accurately.

## CRediT authorship contribution statement

Joseph Dranetz: Writing – review & editing, Writing – original draft, Visualization, Methodology, Formal analysis, Data curation. Shuo Chen: Writing – review & editing, Writing – original draft, Visualization, Methodology, Formal analysis, Data curation. Hwan Choi: Writing – review & editing, Writing – original draft, Supervision, Methodology, Formal analysis, Conceptualization, Project administration, Funding acquisition.

# Declaration of competing interest

The authors declare that they have no known competing financial interests or personal relationships that could have appeared to influence the work reported in this paper.

#### Acknowledgements

This work was supported in part by the National Science Foundation under NSF DARE Program: Award # 2231032 and NSF FRR Program: Award # 2246671.

# Appendix

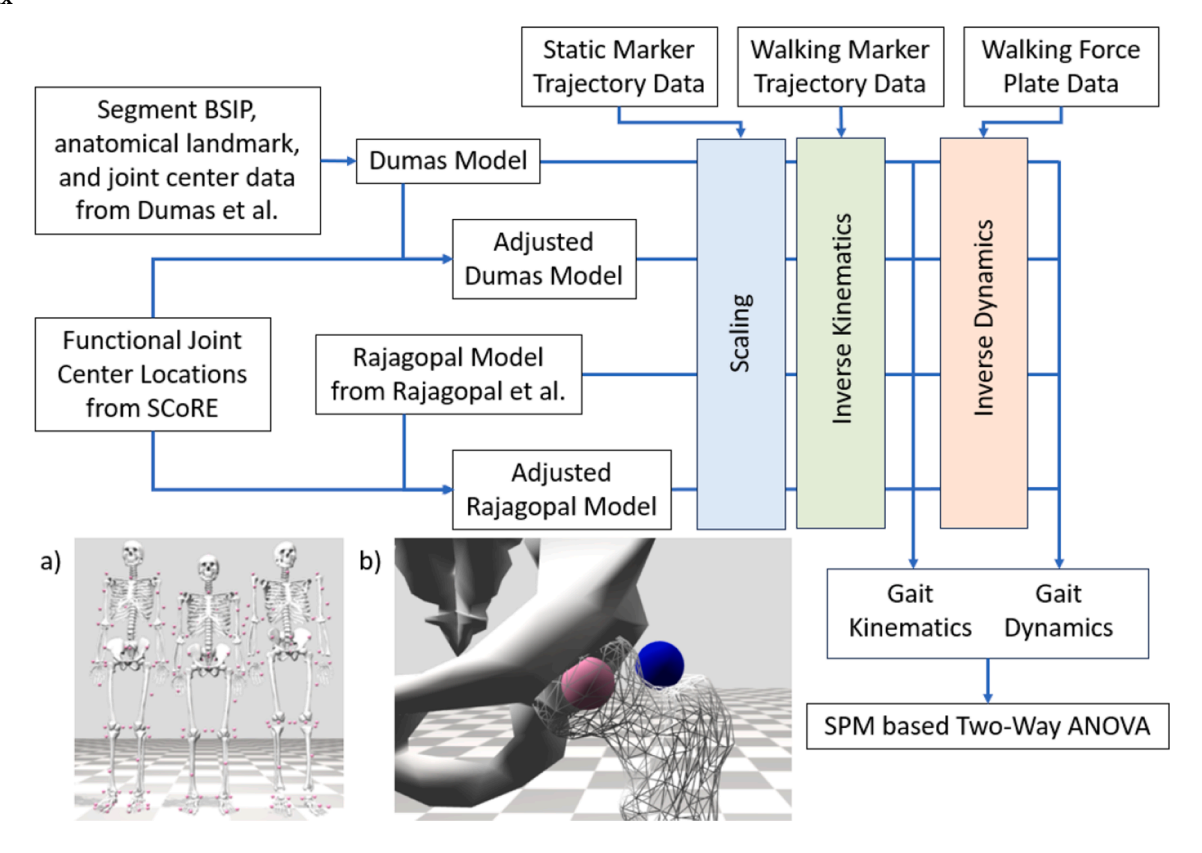


Fig. 4. Schematic overview of study methods. Shows data sources for the 4 models used in the 2x2 SPM based ANOVA as well as treatment of the models. a) Comparison of Rajagopal (left), Female Dumas (middle), and Male Dumas (right) generic models. b) Visual comparison of subject 1's HJC location predicted via scaling of a Rajagopal model (pink) and SCoRE predicted HJC location (blue).

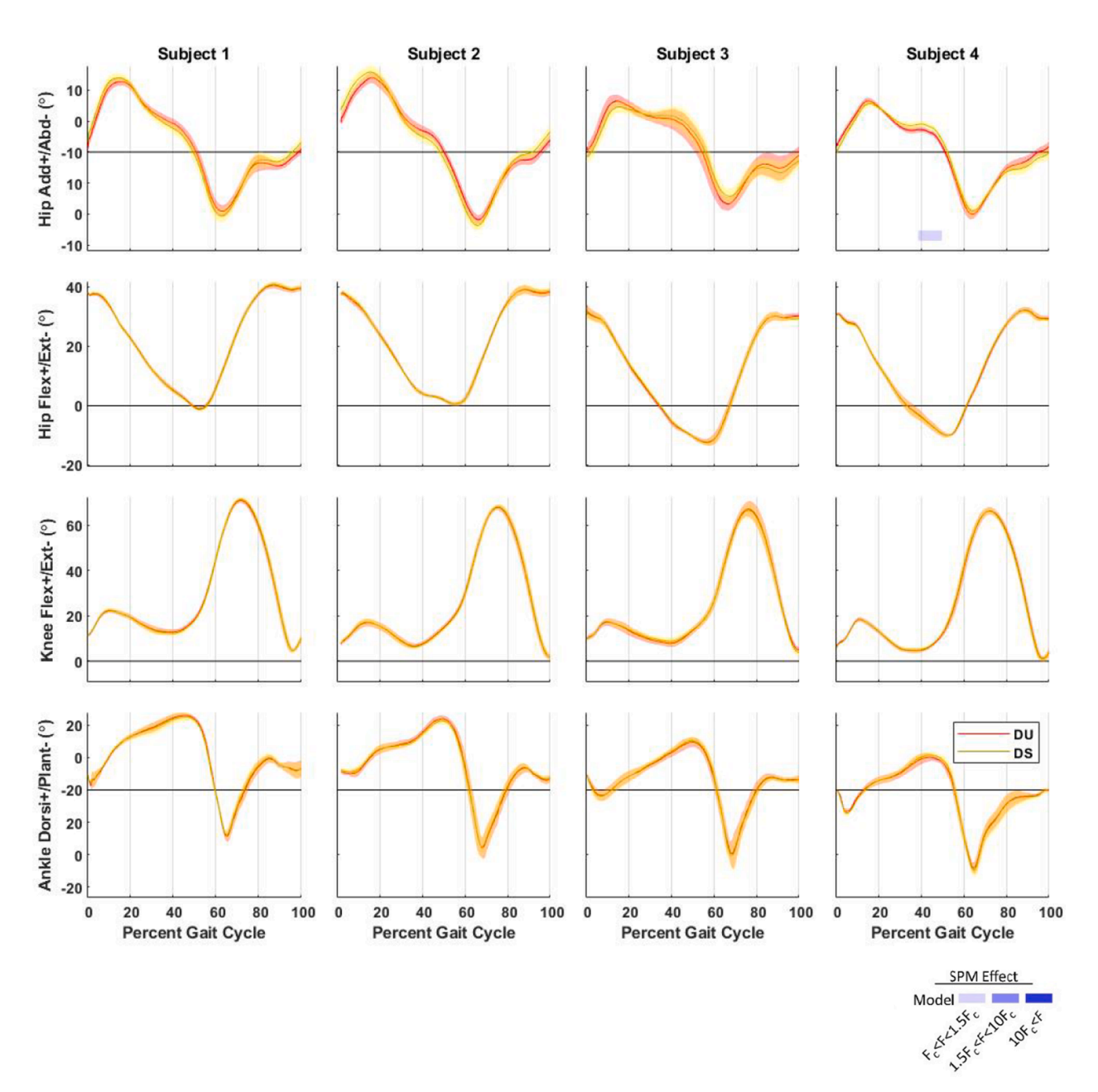


Fig. 5. Kinematics of various joint angles for each subject implementing the scaled gendered Dumas models. DU: Dumas model corresponding with subject sex (same as in Fig. 1), and DS: Dumas model differing from with subject sex. Shaded regions represent the area of  $\pm$  1 standard deviation. The blue boxes below each plot represent regions in the gait cycle identified as having significant differences due to choice in gendered Dumas model.

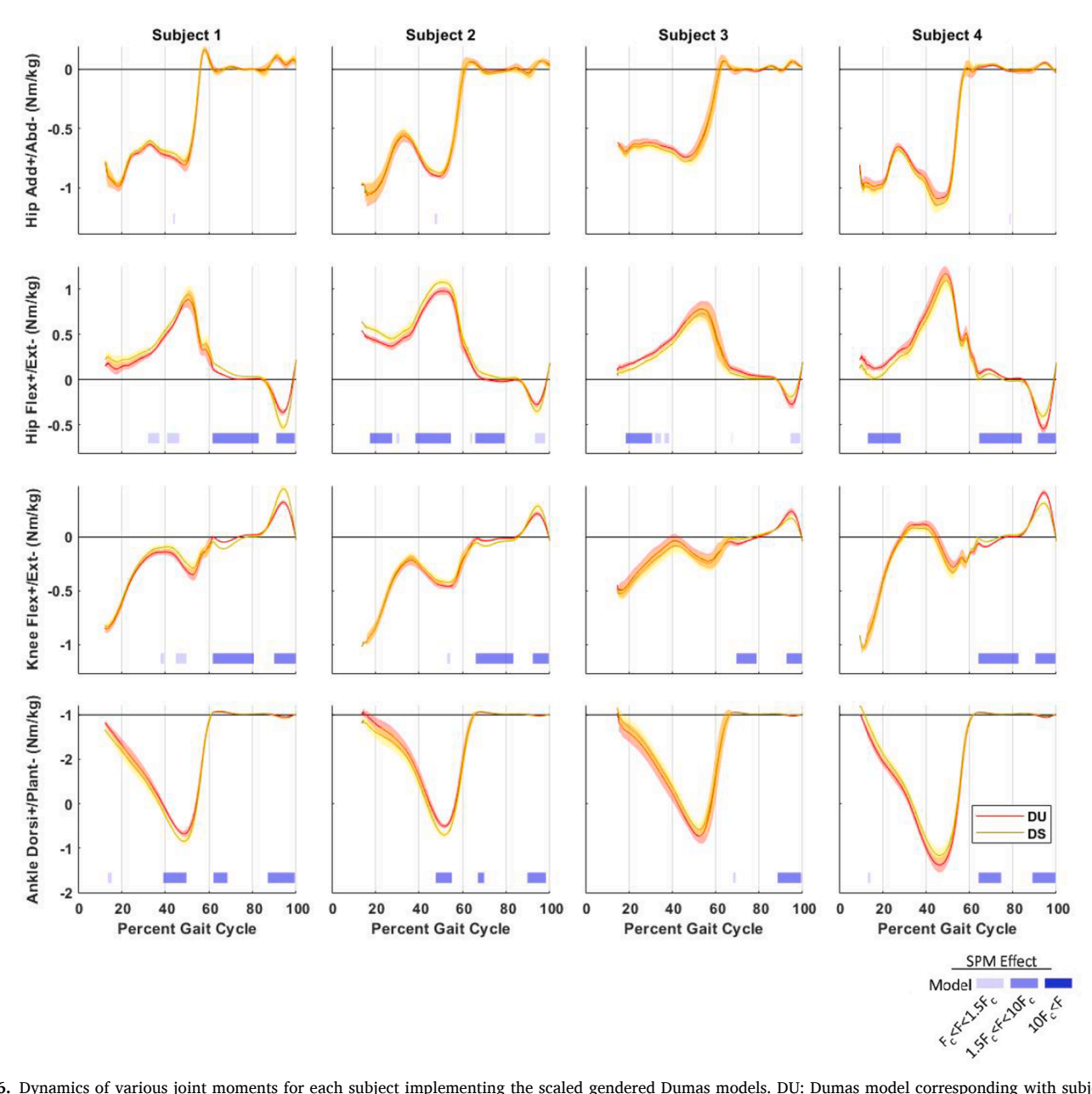


Fig. 6. Dynamics of various joint moments for each subject implementing the scaled gendered Dumas models. DU: Dumas model corresponding with subject sex (same as in Fig. 1), and DS: Dumas model differing from with subject sex. Shaded regions represent the area of  $\pm$  1 standard deviation. The blue boxes below each plot represent regions in the gait cycle identified as having significant differences due to choice in gendered Dumas model.

**Table 4**Model Comparison of Segment Masses (kg).

		Segment Mass	s (kg)		Percent Mass (%)			
Segment	Segment's Coordinate Origin	Rajagopal	Dumas Female	Dumas Male	Rajagopal	Dumas Female	Dumas Male	
Head/Torso	Lumbar Joint Center	26.8266	23.7069	32.2	35.61	36.82	39.65	
Arm	Shoulder Joint Center	2.0325	1.4058	1.932	2.70	2.18	2.38	
Forearm	Elbow Joint Center	1.215	0.8307	1.3685	1.61	1.29	1.69	
Hand	Wrist Joint Center	0.4575	0.3195	0.483	0.61	0.50	0.59	
Pelvis	Anterior Superior Iliac Spine Midpoint	11.777	9.3294	11.431	15.63	14.49	14.08	
Thigh	Hip Joint Center	9.3876	9.3294	9.9015	12.46	14.49	12.19	
Shank	Knee Joint Center	3.705	2.8755	3.864	4.92	4.47	4.76	
Foot	Ankle Joint Center	1.5666	0.915	1.242	2.08	1.42	1.53	
Total		75.332	64.3881	81.213	100	100	100	

Table 5
Model Comparison of Segment Center of Mass (COM) location. Each COM location is defined in the local coordinate system of the segment. The column "Segment's Coordinate Origin" specifies the location of the origin of each of these local coordinate systems.

				COM: Anterior/Pe	osterior [X] (cm)			
Segment	Segment's Coordi	inate Origin		Rajagopal	Dumas Female	Dumas Male		
Head/Torso	Lumbar Joint Cer	nter		-3	-0.84	-1.67		
Arm*	Shoulder Joint Co	enter		0	-1.6	0.5		
Forearm*	Elbow Joint Cent	er		0	0.5	0.3		
Hand*	Wrist Joint Cente	er		0	0.5	0.7		
Pelvis	Anterior Superior	Iliac Spine Midpoint		-7.07	-8.8	-7.5		
Thigh*	Hip Joint Center	• •		0	-2.9	-1.8		
Leg*	Knee Joint Center	r		0	-1.9	-2.1		
Foot*	Ankle Joint Cente	er		6.36	4.5	4.5		
	COM: Superior/Ir	nferior [Y] (cm)		COM: Medial/Lateral [Z] (cm)				
Segment	Rajagopal	Dumas Female	Dumas Male	Rajagopal	Dumas Female	Dumas Male		
Head/Torso	32	29.84	33.34	0	-0.16	-0.08		
Arm*	-16.45	-10.4	-11.8	0	-0.6	-0.7		
Forearm*	-12.05	-10.2	-11.8	0	0.5	0.4		
Hand*	-6.81	-5.5	-6.8	0	0.3	0.6		
Pelvis	0	-1.2	-3.3	0	0	0		
Thigh*	-17	-14.3	-18.5	0	0.3	1.4		
Leg*	-18.67	-15.7	-17.8	0	1.2	0.3		
Foot*	-1.48	-3.6	-3.6	0.51	0.6	0.6		

<sup>\*</sup>Values shown are for features on the right side of the body.

Table 6
Model Comparison of Segment Moment of Inertia (MOI) (units kg×m2).

	Ixx			Iyy			Izz			
Model	Raj	Dum F	Dum M	Raj	Dum F	Dum M	Raj	Dum F	Dum M	
Head/Torso	1.4745	0.6768	0.9854	0.7555	0.2759	0.4013	1.4314	0.6796	1.0231	
Arm*	0.0119	0.0090	0.0136	0.0041	0.0024	0.0028	0.0134	0.0090	0.0145	
Forearm*	0.0066	0.0034	0.0086	0.0025	0.0010	0.0013	0.0071	0.0032	0.0080	
Hand*	0.0009	0.0006	0.0012	0.0005	0.0003	0.0004	0.0013	0.0005	0.0010	
Pelvis	0.1028	0.0885	0.1030	0.0871	0.1068	0.1135	0.0579	0.0667	0.0912	
Thigh*	0.1339	0.1288	0.1554	0.0351	0.0484	0.0416	0.1442	0.1372	0.1663	
Leg*	0.0504	0.0339	0.0568	0.0051	0.0043	0.0072	0.0511	0.0339	0.0568	
Foot*	0.0014	0.0005	0.0009	0.0039	0.0023	0.0044	0.0041	0.0021	0.0042	
				_			_			
34-4-1	Ixy	D F	D M	Ixz	D F	D 14	Iyz	D F	D 14	
Model	Raj	Dum F	Dum M	Raj	Dum F	Dum M	Raj	Dum F	Dum M	
Head/Torso	0	0.1723	0.1950	0	0.0090	0.0023	0	-0.0090	-0.0095	
Arm*	0	0.0001	0.0005	0	-0.0002	0.0004	0	0.0016	0.0001	
Forearm*	0	0.0005	0.0001	0	0.0001	4.4E-5	0	-0.0009	-0.0007	
Hand*	0	0.0001	0.0002	0	0.0001	0.0001	0	-0.0001	-0.0001	
Pelvis	0	-0.0124	-0.0063	0	-1.1E-5	-0.0015	0	-1.1E-5	-0.0007	
Thigh*	0	0.0066	0.0091	0	-0.0005	-0.0007	0	-0.0066	-0.0091	
Leg*	0	0.0002	-0.0012	0	4.3E-5	-0.0003	0	0.0016	0.0018	
Foot*	0	-0.0002	0.0005	0	6.3E-5	-0.0002	0	-2.8E-5	0	

Raj: The Rajagopal Model, Dum F: The Female Dumas Model, Dum M: The Male Dumas Model .

Table 7
Model Comparison of Joint Center Location. Joint center locations are defined relative to the parent's local coordinates. The origin of the child's local coordinate is also defined at the location of the joint center.

				Location: Anterior/Posterior [X] (cm)			
Joint Center	Parent Coordinate	Child C	oordinate	Rajagopal	Dumas Female	Dumas Male	
Lumbar Joint	Pelvis	Torso		-10.07	-8.7	-7.8	
Shoulder Joint*	Torso	Arm		0.32	1.3	2.1	
Elbow Joint*	Arm	Forearr	n	1.31	0	0	
Wrist Joint*	Forearm	Hand		-1.55	0	0	
Hip Joint*	Pelvis	Thigh		-5.63	-3.3	-2.2	
Knee Joint*	Thigh	Shank		-0.81	0	0	
Ankle Joint*	Shank	Foot		-1	0	0	
	Location: Superior/Inferior [Y] (cm)			Location: Medial/Lateral [Z] (cm)			
Joint Center	Rajagopal	Dumas Female	Dumas Male	Rajagopal	Dumas Female	Dumas Male	

(continued on next page)

<sup>\*</sup>Values shown are for features on the right side of the body.

#### Table 7 (continued)

Lumbar Joint	8.15	1.3	-0.7	0	0	0
Shoulder Joint*	37.15	35.4	40.5	17	18.1	20.9
Elbow Joint*	-28.63	-22.95	-26.1	-0.96	0	0
Wrist Joint*	-24.88	-24.7	-28.4	3.97	0	0
Hip Joint*	-7.85	-8	-8.2	7.73	8.8	8.1
Knee Joint*	-40.80	-37.85	-43.15	-0.28	0	0
Ankle Joint*	-40	-38.85	-43.35	0	0	0

<sup>\*</sup>Values shown are for features on the right side of the body.

Table 8

Model Comparison of Anatomical Landmark Marker Locations. Marker locations are defined relative to the local segment coordinates of the segment the marker is attached to.

		Ant./Post. [X] (cm)			Sup./Inf. [Y] (cm)			Med./Lat. [Z] (cm)		
Marker	Origin	Raj.	Dum. F	Dum. M	Raj.	Dum. F	Dum. M	Raj.	Dum. F	Dum. M
C7 Spine	Torso	-8.5	-5.7	-6.9	43.5	46.1	51.2	0.17	0	0
Clavicle	Torso	5.20	4.5	4.6	38.54	38.8	43.3	0	0	0
Acromion*	Torso	0.89	-3	-2.1	43.34	40.5	44.7	17.12	18.1	20.9
Lateral Humeral Epicondyle*	Arm	1.5	0	0	-28	-22.1	-25.8	4	3.4	4.1
Medial Humeral Epicondyle*	Arm	0.22	0	0	-28.6	-23.8	-26.4	-4.6	-3.4	-4.1
Ulnar Styloid*	Forearm	-2.87	0	0	-23.80	-24.2	-28.4	0.41	-2.7	-3.3
Radial Styloid*	Forearm	-0.62	0	0	-23.80	-25.2	-28.4	7.61	2.7	3.3
Anterior Superior Iliac Spine*	Pelvis	3.11	0	0	-0.54	0	0	12.85	11.9	11.2
Posterior Superior Iliac Spine*	Pelvis	-17.93	-19.5	-18	2.73	0	0	4.5	4.6	4.5
Greater Trochanter*	Thigh	-1.75	-1.9	-4	-2.07	0.8	0.6	7.42	8.7	10.1
Lateral Femoral Epicondyle*	Thigh	0	0	0	-40.4	-37.5	-43.1	5.78	5.7	5.7
Medial Femoral Epicondyle*	Thigh	0.39	0	0	-40.40	-38.2	-43.2	-5.35	-5.7	-5.7
Fibular Head*	Shank	-2.33	0	0	-5.74	-4	-2.3	5.59	6	4.7
Lateral Malleolus*	Shank	-1.62	-1	-2.1	-38.36	-39	-43.3	5.94	3.1	3.3
Medial Malleolus*	Shank	0.60	1	2.1	-38.15	-38.7	-43.4	-4.20	-3.1	-3.3
Calcaneus*	Foot	-7.38	-6.9	-5.6	-2.20	-4.6	-2.1	0.29	1.2	0.7
5th Metatarsal*	Foot	8.92	9.7	12.8	-3.69	-4.6	-2.1	7.42	6.2	6.5
1st Toe*	Foot	16.20	17.4	21.9	-2.42	-3.1	-0.4	-1.46	0.9	-0.1

<sup>\*</sup>Values shown are for features on the right side of the body.

#### References

- Abd-Eltawab, A.E., Ameer, M.A., Eladl, M.A., El-Sherbiny, M., Ebrahim, H.A., Elsherbini, D.M., 2022. Sexual dimorphism impact on the ground reaction force acting on the mediolateral direction during level walking: hip abductor muscle biomechanics and its correlation to GRF moment arm. Front. Bioeng. Biotechnol. 10, 863194.
- Anderson, F.C., Pandy, M.G., 1999. A dynamic optimization solution for vertical jumping in three dimensions. Comput. Methods Biomech. Biomed. Eng. 2 (3), 201–231.
- Arnold, E.M., Ward, S.R., Lieber, R.L., Delp, S.L., 2010. A model of the lower limb for analysis of human movement. Ann. Biomed. Eng. 38, 269–279.
- Blemker, S.S., Asakawa, D.S., Gold, G.E., Delp, S.L., 2007. Image-based musculoskeletal modeling: applications, advances, and future opportunities. J. Magn. Reson. Imaging 25 (2). 441–451.
- Camomilla, V., Cereatti, A., Vannozzi, G., Cappozzo, A., 2006. An optimized protocol for hip joint centre determination using the functional method. J. Biomech. 39 (6), 1096–1106.
- Camomilla, V., Cereatti, A., Cutti, A., Fantozzi, S., Stagni, R., 2017. Methodological factors affecting joint moments estimation in clinical gait analysis: a systematic review. Biomed. Eng. Online 16 (1), 1–27.
- Chambers, A.J., Sukits, A.L., McCrory, J.L., Cham, R., 2010. The effect of obesity and gender on body segment parameters in older adults. Clin. Biomech. 25 (2), 131–136.
- Cizgin, P., Kornfeind, P., Haßmann, M., & Baca, A. (2017). Advancements of Methods for Fast and Accurate Estimation of Human Body Segment Parameter Values. Proceedings of the 5th International Congress on Sport Sciences Research and Technology Support. Funchal. Portusal.
- Clauser, C.E., McConville, J.T., Young, J.W., 1969. Weight, Volume, and Center of Mass of Segments of the Human Body. Aerospace Medical Research Laboratory
- Correa, T.A., Baker, R., Graham, H., Pandy, M.G., 2011. Accuracy of generic musculoskeletal models in predicting the functional roles of muscles in human gait. J. Biomech. 44 (11), 2096–2105.
- D'Agostino, R.B., Belanger, A., D'Agostino, R.B., 1990. A suggestion for using powerful and informative tests of normality. Am. Stat. 44 (4), 316–321.
- De Leva, P., 1996. Adjustments to Zatsiorsky-Seluyanov's segment inertia parameters. J. Biomech. 29 (9), 1223–1230.
- Delp, S.L., Loan, J.P., Hoy, M.G., Zajac, F.E., Topp, E.L., Rosen, J.M., 1990. An interactive graphics-based model of the lower extremity to study orthopaedic surgical procedures. IEEE Trans. Biomed. Eng. 37 (8), 757–767.
- Delp, S.L., Anderson, F.C., Arnold, A.S., Loan, P., Habib, A., John, C.T., Thelen, D.G., 2007. OpenSim: open-source software to create and analyze dynamic simulations of movement. IEEE Trans. Biomed. Eng. 54 (11), 1940–1950.

- Derrick, T.R., van den Bogert, A.J., Cereatti, A., Dumas, R., Fantozzi, S., 2020. ISB recommendations on the reporting of intersegmental forces and moments during human motion analysis. J. Biomech. 99, 109533.
- Ding, Z., Tsang, C.K., Nolte, D., Kedgley, A.E., Bull, A.M., 2019. Improving musculoskeletal model scaling using an anatomical atlas: the importance of gender and anthropometric similarity to quantify joint reaction forces. IEEE Trans. Biomed. Eng. 66 (12), 3444–3456.
- Dumas, R., Cheze, L., Verriest, J.P., 2006. Adjustments to McConville et al. and Young et al. body segment inertial parameters. J. Biomech. 40 (3), 543–553.
- Ehrig, R.M., Taylor, W.R., Duda, G.N., Heller, M.O., 2006. A survey of formal methods for determining the centre of rotation of ball joints. J. Biomech. 39 (15), 2798–2809.
- Fernandez, J., Shim, V., Schneider, M., Choisne, J., Handsfield, G., Yeung, T., Besier, T., 2023. A narrative review of personalized musculoskeletal modeling using the physiome and musculoskeletal atlas projects. J. Appl. Biomech. 39 (5), 304–317.
- Fiorentino, N.M., Kutschke, M.J., Atkins, P.R., Foreman, K.B., Kapron, A.L., Anderson, A. E., 2016. Accuracy of functional and predictive methods to calculate the hip joint center in young non-pathologic asymptomatic adults with dual fluoroscopy as a reference standard. Ann. Biomed. Eng. 44, 2168–2180.
- Ganley, K.J., Powers, C.M., 2004. Determination of lower extremity anthropometric parameters using dual energy x-ray absorptiometry: the influence on net joint moments during gait. Clin. Biomech. 19 (1), 50–56.
- Hamner, S.R., Seth, A., Delp, S.L., 2010. Muscle contributions to propulsion and support during running. J. Biomech. 43 (14), 2709–2716.
- Holder, J., Trinler, U., Meurer, A., Stief, F., 2020. A systematic review of the associations between inverse dynamics and musculoskeletal modeling to investigate joint loading in a clinical environment. Front. Bioeng. Biotechnol. 8, 603907.
- Inman, V.T., 1976. The Joints of the Ankle. Williams & Wilkins.
- Kadaba, M.P., Ramakrishnan, H.K., Wootten, M.E., 1990. Measurement of lower extremity kinematics during level walking. J. Orthop. Res. 8 (3), 383–392.
- Kainz, H., Carty, C.P., Modenese, L., Boyd, R.N., Lloyd, D.G., 2015. Estimation of the hip joint centre in human motion analysis: a systematic review. Clin. Biomech. 30 (4), 319–329
- Kainz, H., Hajek, M., Modenese, L., Saxby, D.J., Lloyd, D.G., Carty, C.P., 2017. Reliability of functional and predictive methods to estimate the hip joint centre in human motion analysis in healthy adults. Gait Posture 53, 179–184.
- Kainz, H., Wesseling, M., Jonkers, I., 2021. Generic scaled versus subject-specific models for the calculation of musculoskeletal loading in cerebral palsy gait: effect of personalized musculoskeletal geometry outweighs the effect of personalized neural control. Clin. Biomech. 87, 105402.
- Koller, W., Baca, A., Kainz, H., 2021. Impact of scaling errors of the thigh and shank segments on musculoskeletal simulation results. Gait Posture 87, 65–74.

- Kowalski, E., Catelli, D.S., Lamontagne, M., 2021. A waveform test for variance inequality, with a comparison of ground reaction force during walking in younger vs. older adults. J. Biomech. 127, 110657.
- Krabbe, B., Farkas, R., Baumann, W., 1997. Influence of inertia on intersegment moments of the lower extremity joints. J. Biomech. 30 (5), 517–519.
- Kudzia, P., Jackson, E., Dumas, G., 2022. Estimating body segment parameters from three-dimensional human body scans. PLoS One 17 (1), e0262296.
- Langenderfer, J.E., Laz, P.J., Petrella, A.J., Rullkoetter, P.J., 2008. An efficient probabilistic methodology for incorporating uncertainty in body segment parameters and anatomical landmarks in joint loadings estimated from inverse dynamics. J. Biomech. Eng. 130 (1), 014502.
- Lund, M.E., Andersen, M.S., de Zee, M., Rasmussen, J., 2015. Scaling of musculoskeletal models from static and dynamic trials. Int. Biomech. 2 (1), 1–11.
- McConville, J.T., Clauser, C.E., Churchill, T.D., Cuzzi, J., Kaleps, I., 1980.

  Anthropometric Relationships of Body and Body Segment Moments of Inertia. Air Force Aerospace Medical Research Laboratory, Yellow Springs, Ohio.
- Miehling, J., 2019. Musculoskeletal modeling of user groups for virtual product and process development. Comput. Methods Biomech. Biomed. Eng. 22 (15), 1209–1218.
- Modenese, L., Renault, J.B., 2021. Automatic generation of personalised skeletal models of the lower limb from three-dimensional bone geometries. J. Biomech. 116, 110186.
- Moissenet, F., Modenese, L., Dumas, R., 2017. Alterations of musculoskeletal models for a more accurate estimation of lower limb joint contact forces during normal gait: a systematic review. J. Biomech. 63, 8–20.
- Myers, C.A., Laz, P.J., Shelburne, K.B., Davidson, B.S., 2015. A probabilistic approach to quantify the impact of uncertainty propagation in musculoskeletal simulations. Ann. Biomed. Eng. 43, 1098–1111.
- Nguyen, T.C., Reynolds, K.J., 2014. The effect of variability in body segment parameters on joint moment using Monte Carlo simulations. Gait Posture 39 (1), 346–353.
- Pataky, T.C., Robinson, M.A., Vanrenterghem, J., 2016. Region-of-interest analyses of one-dimensional biomechanical trajectories: bridging 0D and 1D theory, augmenting statistical power. *Peerj* 4, e2652.
- Peyer, K.E., Morris, M., Sellers, W.I., 2015. Subject-specific body segment parameter estimation using 3D photogrammetry with multiple cameras. PeerJ 3, e831.
- Puchaud, P., Sauret, C., Muller, A., Bideau, N., Dumont, G., Pillet, H., Pontonnier, C., 2020. Accuracy and kinematics consistency of marker-based scaling approaches on a lower limb model: a comparative study with imagery data. Comput. Methods Biomech. Biomed. Eng. 23 (3), 114–125.
- Rajagopal, A., Dembia, C.L., DeMers, M.S., Delp, D.D., Hicks, J.L., Delp, S.L., 2016. Full-body musculoskeletal model for muscle-driven simulation of human gait. IEEE Trans. Biomed. Eng. 63 (10), 2068–2079.

- Rao, G., Amarantini, D., Berton, E., Favier, D., 2006. Influence of body segments' parameters estimation models on inverse dynamics solutions during gait. J. Biomech. 39 (8), 1531–1536.
- Reed, M. P., Manary, M. A., & Schneider, L. W. (1999). Methods for Measuring and Representing Automobile Occupant Posture. In U. o. Institute (Ed.), University of Michigan Transportation Research Institute. Detroit, Michigan: Society of Automotive Engineers Inc.
- Sangeux, M., Pillet, H., Skalli, W., 2014. Which method of hip joint centre localisation should be used in gait analysis? Gait Posture 40 (1), 20–25.
- Seth, A., Sherman, M., Reinbolt, J.A., Delp, S.L., 2011. OpenSim: a musculoskeletal modeling and simulation framework for in silico investigations and exchange. Proc. IUTAM 2, 212–232.
- Stagni, R., Leardini, A., Cappozzo, A., Benedetti, M.G., Cappello, A., 2000. Effects of hip joint centre mislocation on gait analysis results. J. Biomech. 33 (11), 1479–1487
- Sunil Kumar, K.H., Rawal, J., Nakano, N., Sarmento, A., Khanduja, V., 2021.

  Pathogenesis and contemporary diagnoses for lateral hip pain: a scoping review.

  Knee Surg. Sports Traumatol. Arthoscopy 29 (8), 2408–2416.
- Toderita, D., Henson, D.P., Klemt, C., Ding, Z., Bull, A.M., 2021. An anatomical atlas-based scaling study for quantifying muscle and hip joint contact forces in above and through-knee amputees using validated musculoskeletal modelling. IEEE Trans. Biomed. Eng. 68 (11), 3447–3456.
- Valente, G., Crimi, G., Vanella, N., Schileo, E., Taddei, F., 2017. nmsBuilder: freeware to create subject-specific musculoskeletal models for OpenSim. Comput. Methods Programs Biomed. 152, 85–92.
- Wesseling, M., De Groote, F., Jonkers, I., 2014. The effect of perturbing body segment parameters on calculated joint moments and muscle forces during gait. J. Biomech. 47 (2), 596–601.
- Wu, G., Van der Helm, F.C., Veeger, H.D., Makhsous, M., Van Roy, P., Anglin, C., Wang, X., 2005. ISB recommendation on definitions of joint coordinate systems of various joints for the reporting of human joint motion. J. Biomech. 38 (5), 981–992.
- Young, J.W., Chandler, R.F., Snow, C.C., Robinette, K.M., Zehner, G.F., Lofberg, M.S., 1983. Anthropometric and Mass Distribution Characteristics of the Adult Female. FAA Civil Aeromedical Institute, Oklahoma City, Oklahoma.
- Zatsiorski, V., Seluyanov, V., Chugunova, L., 1990. In vivo body segment inertial parameters determination using Gamma-Scanner method. Biomech. Human Movement 186–202.
- Zhang, J., Sorby, H., Clement, J., Thomas, C.D., Hunter, P., Nielsen, P., Besier, T., 2014. The MAP Client: User-Friendly Musculoskeletal Modelling Workflows. *International Symposium on Biomedical Simulation*. Springer International Publishing, Cham, Germany.
- Zhang, J., Fernandez, J., Hislop-Jambrich, J., Besier, T.F., 2016. Lower limb estimation from sparse landmarks using an articulated shape model. J. Biomech. 49 (16), 3875–3881.